Barrel-Type Distortion Compensated Fourier Feature Extraction

Michael Gadermayr, Andreas Uhl, and Andreas Vécsei

[1] Department of Computer Sciences, University of Salzburg, Austria
{mgadermayr,uhl}@cosy.sbg.ac.at
[2] St.Anna Children's Hospital, Endoscopy Unit, Vienna, Austria

Abstract. Fourier based feature extraction is a common and powerful technique used in texture classification. In case of endoscopic imaging, often significant barrel-type distortions affect the feature extraction. Although images can be rectified using distortion correction techniques, in previous work feature extraction proved to suffer not just from geometric distortions, but also from effects within distortion correction. Distortion correction in combination with Fourier features has not been investigated so far. We introduce and evaluate three strategies to partially or completely compensate the geometric distortion in combination with Fourier features. With two methods, the interpolation within distortion correction can be omitted which should lead to a benefit in classification. Instead of making a general statement, we distinguish between certain frequencies and identify the positive and the negative aspects of the strategies.

1 Introduction

The computer aided diagnosis of celiac disease relies on images taken during endoscopy. The utilized cameras are equipped with wide angle lenses, which significantly suffer from barrel-type distortion. Especially in peripheral image regions significant degradations can be observed. This potentially affects the feature extraction as well as the following classification. Distortion correction (DC) techniques are able to rectify the images. For computer aided celiac disease diagnosis, reliable 128×128 pixel patches are extracted in a manual way from these images for further processing.

In recent work [1–4], the impact of barrel type distortions and distortion correction on the classification accuracy of celiac disease endoscopy images has been investigated. In [2] the authors showed that image patches in (stronger affected) peripheral regions are more likely to be misclassified. However, the achieved classification rates in most cases do not benefit from the distortion correction. Whereas the images are geometrically rectified, the required image stretching in combination with interpolation leads to new problems in texture classification. Especially in peripheral regions the images are blurred because of the high degree of image stretching. Whereas the stretching cannot be circumvented within image rectification, the interpolation stage can.

Experiments showed that even (very) low dimensional Fourier features are highly discriminative in the case of celiac disease classification. Therefore, in this work, we investigate different ways of extracting barrel-type distortion corrected Fourier features. Apart from the traditional DC approach (as investigated in [1–4] with various other features) based on previously rectified images, we introduce two additional techniques especially developed for Fourier features. One method is based on the non-uniform discrete Fourier transform (NDFT) [5], in order to omit the interpolation step. The other one utilizes the traditional discrete Fourier transform (DFT) and distorted images to finally correct the Fourier domain data. We anticipate a positive effect of DC especially with lower Fourier frequencies, as these frequencies are majorly affected by the distortions. The two new methods, which are not based on pixel interpolations, are expected to improve the discriminative power further more. In experiments, the competitiveness of various approaches is compared. To make a general statement, we separately consider the discriminative power in different frequency bands. Moreover, we apply a feature subset selection to identify advantageous feature combinations.

The paper is organized as follows: In Sect. 2, two new DC Fourier feature extraction techniques are introduced. In Sect. 3, experiments are shown and the results are discussed. Section 4 concludes this paper.

2 Fourier-Based Feature Extraction

In this section, we explain three methods to extract Fourier features in a way to maintain the geometrical correctness (DCF0, DCF1 and DCF2) and the most straight-forward NDC method without a distortion correction.

2.1 NDC: Feature Extraction Without DC

The simplest way of dealing with barrel-type distorted images is, to simply ignore the distortion. In [6, 7] Fourier features are extracted from endoscopic images, without considering any distortion compensation.

2.2 DCF0: Traditional DC Followed by DFT

As there exists many different DC-models, first one of them has to be chosen, and the distortion parameters must be estimated. For simplicity, we concentrate on the distortion correction method of Melo et al. [8], which proved to be appropriate for our requirements. In this approach, the circular barrel-type distortion is modeled by the division model [9]. Having the center of distortion $\hat{x}_c$ and the distortion parameter ξ, an undistorted point x_u can be calculated from the distorted point x_d as follows:

$$x_u = \hat{x}_c + \frac{(x_d - \hat{x}_c)}{||x_d - \hat{x}_c||_2} \cdot r_u(||x_d - \hat{x}_c||_2) \; . \tag{1}$$

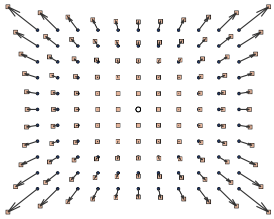

Fig. 1: Irregular grid (squares) achieved by applying Eq. (1) on the distorted image points (round points).

$||x_d - \hat{x}_c||_2$ (in the following r_d) is the distance (radius) of the distorted point x_d from the center of distortion $\hat{x}_c$. The function r_u defines for a radius r_d in the distorted image, the new radius in the undistorted image:

$$r_u(r_d) = \frac{r_d}{1 + \xi \cdot r_d^2} \ . \tag{2}$$

To get the distortion corrected image, for each (discrete) undistorted point x_u in the new undistorted image, the corresponding distorted point x_d in the distorted image has to be computed. However, a remaining issue is that x_d is not necessarily a discrete point. Consequently, an interpolation method has to be applied, in order to get image values for continuous points.

In [1–4], this traditional DC method has been investigated with various feature extraction techniques. However, to the best of our knowledge the effect of DC on Fourier features has not been investigated so far.

2.3 DCF1: DC Followed by Non-Uniform DFT

The investigations of the traditional DC method [1–4] showed that the classification performance often suffers from DC. Obviously, the interpolation leads to a loss of discriminative power and the benefits of geometrical corrections disappear. In order to omit the interpolation step, we replace the DFT by the non-uniform discrete Fourier transform [5] (NDFT). Instead of creating an undistorted image separately from Fourier transform, now we combine the image rectification and the feature extraction stage. The following steps are applied:

1. All points x_d in the distorted image are undistorted using Eq. (1). This results in an irregular grid as shown in Fig. 1.
2. Next the NDFT is applied to the irregular grid and we achieve the frequency domain data:
$$F(u,v) = \sum_{j=0}^{N-1} f_j \cdot e^{-2\pi i (u,v)\cdot p_j} \ . \tag{3}$$
N is the number of sample points, f_j are the image values and p_j are the corresponding corrected coordinates (squares in Fig. 1).

The advantage of this strategy is that no interpolation must be applied, which turned out to be disadvantageous in previous work.

2.4 DCF2: DFT Followed by Affine Correction of Fourier Coefficients

Another way to (partially) correct the distortion is to transform data into Fourier domain and afterwards correct the distortion in the frequency domain.

The affine theorem [10] gives us a connection between the affine transformed spatial domain and the affine transformed frequency domain data. If $f(x, y)$ has the Fourier coefficients $F(u, v)$ then the affine transformed $g(x, y) = f(ax + by + c, dx + ey + c)$ has the Fourier coefficients:

$$G(u,v) = \frac{1}{|\Delta|} \cdot e^{\frac{2\pi i}{\Delta}[(e \cdot c - b \cdot f) \cdot u + (a \cdot f - c \cdot d) \cdot v]} \cdot F\left(\frac{e \cdot u - d \cdot v}{\Delta}, \frac{a \cdot v - b \cdot u}{\Delta}\right) , \quad (4)$$

where

$$\Delta = a \cdot e - b \cdot d \; . \quad (5)$$

As barrel-type distortion cannot be modeled by an affine transformation, using the affine theorem a precise rectification cannot be achieved. However, as we do not consider the whole image for feature extraction, but only small patches, the barrel-type DC of the patches can be modeled approximately with an affine transformation.

We apply the following steps:

1. First employ the traditional DFT on the distorted image.
2. Compute the best fitting affine transformation:

   (a) Undistort the 4 corner points of the square image patch.
   (b) Compute the best fitting parallelogram in a least squares sense.
   (c) Calculate the affine matrix to transform the ideal square patch into the achieved parallelogram.
3. Directly "undistort" the Fourier coefficients with the parameters of the calculated best fitting affine transformation according to the affine theorem.

In Fig. 2, the Fourier power spectra achieved with the different approaches applied to an example image patch are shown. The patch has been extracted in a quite commonly distorted image area. It can be observed that with the distortion correction (especially DCF0 and DCF2), the higher frequencies are decreasing. With DCF2, large ranges are even set to zero. With DCF1, a similar behavior cannot be observed. This is due to the aliasing effects occurring with this method.

3 Experiments

3.1 Experimental Setup

The image test set used contains images of the Duodenal Bulb taken during duodenoscopies at the St. Anna Children's Hospital using pediatric gastroscopes (with resolution 768×576 and 528×522 pixels, respectively).

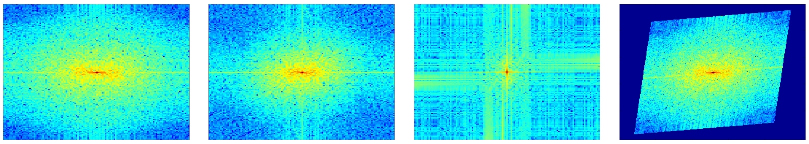

(a) NDC (b) DCF0 (c) DCF1 (d) DCF2

Fig. 2: Example Fourier power spectra achieved with the different approaches.

In a preprocessing step, texture patches with a fixed size of 128×128 pixels were extracted in a manual fashion (see Fig. 3). In case of distortion correction, the new patch position (the patch center) is adjusted according to the distortion function. Within traditional DC (DCF0), bi-linear interpolation is utilized. Experiments with other interpolation methods did not lead to significantly different results. For all of our experiments, the patches are converted to gray value images. To generate the ground truth for the texture patches used, the condition of the mucosal areas covered by the images was determined by histological examination of biopsies from the corresponding regions. Severity of villous atrophy was classified according to the modified Marsh classification [11]. Although it is possible to distinguish between the different stages of the disease. we only aim in distinguishing between images of patients with (Marsh 3A-3C) and without the disease (Marsh 0). Our experiments are based on a database containing 163 (Marsh 0) and 124 (Marsh 3A-3C) images, respectively. For classification, the k-nearest neighbor classifier is used in combination with leave-one-patient-out cross validation. In order to get stable results and to prevent from over-fitting, the rates achieved for k reaching from 1 to 30 are averaged.

We separately investigate the discriminative power of the mean (MEAN), the median (MEDIAN) and the variance (VAR) of the Fourier power spectrum within specific frequency ranges. Each frequency range corresponds to a ring in the Fourier domain image. Each ring has a thickness of 2 pixels (thereby the number of coefficients varies). This methodology is applied, as we do not want to be restricted to our specific problem definition. We would like to get an overview of the preservation of specific frequencies with the different DC methods. Not the highest overall rates are of our interest, but relatively high rates in a specific frequency range.

(a) Marsh 3A-3C (disease is present) (b) Marsh 0 (disease is not present)

Fig. 3: Example patches of patients with (a) and without the disease (b).

In order to get higher rates and to identify advantageous combinations of features, we further apply a feature subset selection. Although there definitely exist more sophisticated approaches, we compute all classification rates of subsets of size 2 - to get a large amount of data for analysis. Considering larger sizes (above 2) in combination with more sophisticated subset selection approaches, we did not achieve significantly better classification rates.

3.2 Results

Single Features In the following plots (Fig. 4), for each frequency band (x-axis), the achieved classification rate (y-axis) is given for all feature extraction variations DCF0-2 and NDC. On the x-axis the average radius r of the frequency ring is given (i.e. the frequency range is given by the interval $[r-1, r+1)$).

In Fig. 4a, the results achieved with the MEAN feature are given. Considering low frequencies (below 8), the performances of the DC-approaches are in each case better than the NDC approach, which is not based on DC. Especially the approximative DCF2 approach performs best with the low frequencies. With higher frequencies (above 9), the behavior is inverted and the NDC approach is (slightly) better than the others. When frequencies become very high, all DC approaches are inferior to the NDC approach. The best overall rates are achieved with the NDC and the DCF0 method.

Figure 4b shows the results of the the quite similar MEDIAN feature. As anticipated, a similar behavior is achieved, however, when considering the best overall rates, the DC approaches profit from the properties of the median by tendency. With higher frequencies, NDC provides the best discriminative power.

In Fig. 4c, the results achieved with the VAR feature are given. With VAR, especially DCF1 is not able to keep up with the others, even in low frequency bands. Considering high frequencies (above 46), interestingly the interpolation based DCF0 approach, is even able to outreach NDC. With very low frequencies, DCF2 again delivers the best rates.

Feature Subset Selection In Fig. 5, the results of the feature subset selection are presented. All combinations of the features MEAN, MEDIAN and VAR and of the 4 feature extraction strategies NDC DCF0 DCF1 and DCF2 from the frequencies as in Fig. 4a - 4c have been evaluated.

Figure 5a shows for each pair of strategies, the number of beneficial pairs, weighted (i.e. multiplied) with the respective improvement. A pair of configurations is defined to be beneficial, if the best rate of a single feature (88.59 %, achieved with MEDIAN and DCF0) is outreached. The improvement is the difference to this value. We decided for this visualization strategy as the differences are quite small and we do not want to overvalue insignificant changes (especially as we do not have a separate validation-set).

Figure 5b shows for each pair of strategies, the maximum achieved classification rate. Actually, it is not totally fair to compare these values, with rates achieved with single features (as these rates are maximized). However, we can

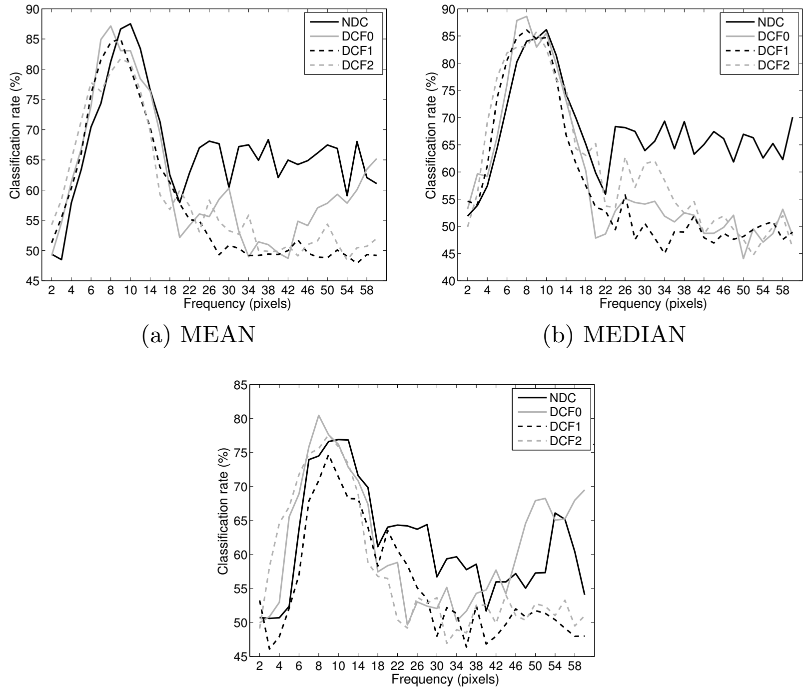

(a) MEAN (b) MEDIAN

(c) VAR

Fig. 4: Experimental results achieved with the different feature extraction extraction ((a) – (c)) and distortion correction methods (see legend).

cope with this inadequacy as we mainly aim in identifying good feature combinations.

In Fig. 5c and 5d, the results of the best combinations (MEDIAN: DCF0/DCF0 (c) and DCF0/DCF2 (d)) are shown with reference to the respective frequencies. The best feature pairs (rates $> 90\%$) are marked with a cross.

The best overall results for a single feature are achieved with the MEDIAN/DCF0 setup. If we consider combinations of 2 features, again this setup seems to be quite competitive. The most and the highest improvements are gathered in combination with MEDIAN/DCF2 and MEDIAN/DCF0 (which is the same configuration again). For exhaustiveness, the best achieved rates and the respective configurations are given in Table 1. The best rates are prevailingly achieved with frequencies between 6 and 12.

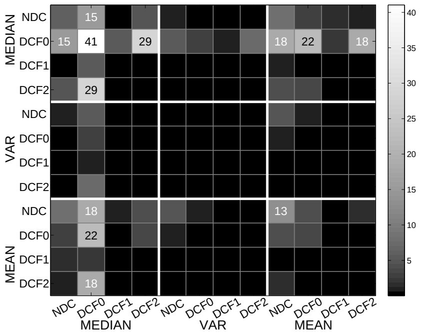

(a) Weighted number of improvements compared to the best single feature rate. All numbers above 10 are given.

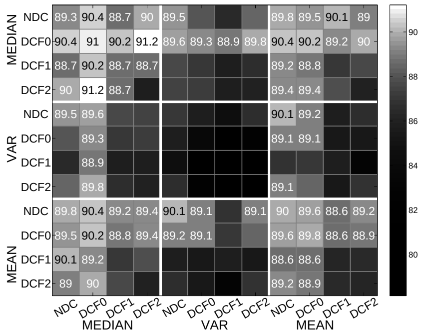

(b) Maximum achieved rate, for each combination. The Rate is given in case of an improvement.

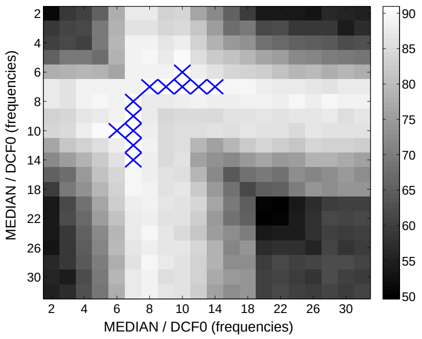

(c) Detailed Results: MEDIAN/DCF0 combined with MEDIAN/DCF0

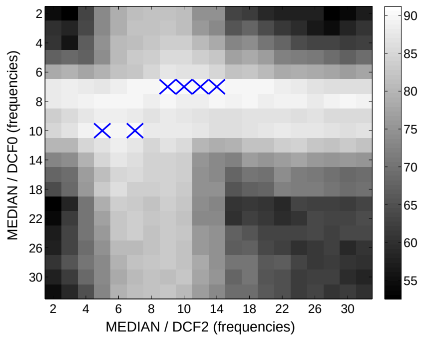

(d) Detailed Results: MEDIAN/DCF0 combined with MEDIAN/DCF2

Fig. 5: Various visualizations of classification rates achieved with feature subset selection. An overview is given in (a) and (b) and details for most beneficial combinations are presented in (c) and (d).

3.3 Discussion

We will separately discuss the effects of the following inadequacies:

- Barrel-type distortions (prevalent in NDC)
- Interpolation within DC (prevalent in DCF0)
- Image stretching within DC (prevalent in DCF0, DCF1 and DCF2)

In the following, we will not focus on DCF1. Although this method is quite competitive with low frequencies (MEAN and MEDIAN), it suffers from strong aliasing artifacts. The bad performance in the high frequency range as well as the disadvantageous behavior with VAR are due to this problem. Considering high frequencies (> 20), NDC on average is the best choice. Obviously, in this range, the barrel-type distortions are less disadvantageous than the effects of stretching (and interpolation) within DC. Interestingly, the additional interpolation step

Table 1: Configurations of the highest classification rates with subsets of size 2.

Feature 1			Feature 2			
Feature	DC Approach	Frequency	Feature	DC Approach	Frequency	Rate
MEDIAN	DCF0	7	MEDIAN	DCF2	9	91.21
MEDIAN	DCF0	6	MEDIAN	DCF0	10	90.99
MEDIAN	DCF0	7	MEDIAN	DCF0	11	90.91
MEDIAN	DCF0	7	MEDIAN	DCF0	10	90.51
MEDIAN	DCF0	7	MEDIAN	DCF0	12	90.46

seems to be not disadvantageous, as DCF0 is slightly more competitive than DCF2. However, we anticipated a bad behavior of DCF2, as the affine theorem leads to a lack of high frequencies, especially in case of strong distortions (see Fig. 2d). Considering very low frequencies, especially DCF2 robustly delivers the best classification performance, followed by the other DC-based methods. In this range, not just the distortion correction, but also the omission of the interpolation actually leads to a higher discriminative power. The positive effect of DC outweighs the negative ones. The most straight forward DCF0 on average performs best in a quite small frequency range (around 8). However, in case of celiac disease classification, these bands are the most discriminative ones. Interestingly, in this range, DCF2 is less competitive. We assume, this is due to the approximative nature of this approach. As the distortion of a patch is modeled by an affine transform, especially in highly distorted peripheral regions, an inaccuracy is introduced. For other problem definitions, where lower frequencies are more discriminative, we anticipate a slightly higher competitiveness of DCF2 compared to the other methods. If higher frequencies were more discriminative, we would recommend to utilize the NDC approach being not based on DC. With feature subset selection, again DCF0 turned out to be the best choice for our problem definition. Most competitive rates are achieved with combinations consisting of 2 median features based on DCF0. Interestingly, the combination of e.g. DCF0 and NDC based features as well as the combination of MEDIAN and MEAN or VAR does not lead to improvements. Obviously, although we use quite different feature extraction methods in combination with different DC techniques, the computed features are significantly correlated.

4 Conclusion

In this work, we present different ways to get (distortion corrected) Fourier features each having its advantages and disadvantages. Within the high frequency bands, the negative effects of image rectification prevail over the positive ones. Here, the discriminative power even does not benefit from the omission of interpolation. As expected, we observed that distortion correction has a positive effect in features extracted from lower frequency bands. Within very low frequency bands, not just distortion correction, but also the omission of interpolation (DCF2) seems to be beneficial. However, for this specific problem definition, DCF0 in combination with the MEDIAN feature and with traditional distortion correction delivers the best classification results. With feature subset selection, the classification rates can be improved. The most and the highest improvements are achieved with combinations of MEDIAN and DCF0.

Acknowledgment This work is partially funded by the Austrian Science Fund (FWF) under Project No. 24366.

References

1. Gschwandtner, M., Liedlgruber, M., Uhl, A., Vécsei, A.: Experimental study on the impact of endoscope distortion correction on computer-assisted celiac disease diagnosis. In: Proceedings of the 10th International Conference on Information Technology and Applications in Biomedicine (ITAB'10), Corfu, Greece (November 2010)
2. Liedlgruber, M., Uhl, A., Vécsei, A.: Statistical analysis of the impact of distortion (correction) on an automated classification of celiac disease. In: Proceedings of the 17th International Conference on Digital Signal Processing (DSP'11), Corfu, Greece (July 2011)
3. Gschwandtner, M., Hämmerle-Uhl, J., Höller, Y., Liedlgruber, M., Uhl, A., Vécsei, A.: Improved endoscope distortion correction does not necessarily enhance mucosa-classification based medical decision support systems. In: Proceedings of the IEEE International Workshop on Multimedia Signal Processing (MMSP'12). (September 2012) 158–163
4. Hämmerle-Uhl, J., Höller, Y., Uhl, A., Vécsei, A.: Endoscope distortion correction does not (easily) improve mocusa-based classification of celiac disease. In: Medical Image Computing and Computer-Assisted Intervention – MICCAI 2012. Volume 7512 of Springer Lecture Notes in Computer Science. (September 2012) 574–581
5. Bagchi, S., Mitra, S.K.: The nonuniform discrete Fourier transform and its applications in signal processing. Kluwer Academic Publishers, Norwell, MA, USA (1999)
6. Vécsei, A., Fuhrmann, T., Liedlgruber, M., Brunauer, L., Payer, H., Uhl, A.: Automated classification of duodenal imagery in celiac disease using evolved fourier feature vectors. Comp. Meth. and Programs in Biomedicine **95** (2009) S68 – S78
7. Häfner, M., Brunauer, L., Payer, H., Resch, R., Wrba, F., Gangl, A., Vécsei, A., Uhl, A.: Pit pattern classification of zoom-endoscopic colon images using DCT and FFT. In Kokol, P., Podgorelec, V., Micetic-Turk, D., Zorman, M., Verlic, M., eds.: Proc. of the IEEE Intern. Symp. on Computer-Based Medical Systems (CBMS'07), Maribor, Slovenia, IEEE Computer Society CPS (June 2007) 159–164
8. Melo, R., Barreto, J.P., Falcao, G.: A new solution for camera calibration and real-time image distortion correction in medical endoscopy-initial technical evaluation. IEEE Trans Biomed Eng. **59**(3) (2012) 634–44
9. Fitzgibbon, A.W.: Simultaneous linear estimation of multiple view geometry and lens distortion. In: CVPR. (2001) 125–132
10. Bracewell, R., Chang, K.Y., Jha, A., Wang, Y.H.: Affine theorem for two-dimensional fourier transform. Electronics Letters **29**(3) (feb. 1993) 304
11. Oberhuber, G., Granditsch, G., Vogelsang, H.: The histopathology of coeliac disease: time for a standardized report scheme for pathologists. European Journal of Gastroenterology and Hepatology **11** (nov 1999) 1185–1194